

# CsOx Nanostructures on Au(111): Morphology- and Size-dependent Activity for the Water-Gas Shift Reaction

R. Shi, J. A. Rodriguez

To be published in "The Journal of Physical Chemistry C"

February 2024

Chemistry Department  
**Brookhaven National Laboratory**

**U.S. Department of Energy**  
USDOE Office of Science (SC), Basic Energy Sciences (BES)

Notice: This manuscript has been authored by employees of Brookhaven Science Associates, LLC under Contract No. DE-SC0012704 with the U.S. Department of Energy. The publisher by accepting the manuscript for publication acknowledges that the United States Government retains a non-exclusive, paid-up, irrevocable, world-wide license to publish or reproduce the published form of this manuscript, or allow others to do so, for United States Government purposes.

## **DISCLAIMER**

This report was prepared as an account of work sponsored by an agency of the United States Government. Neither the United States Government nor any agency thereof, nor any of their employees, nor any of their contractors, subcontractors, or their employees, makes any warranty, express or implied, or assumes any legal liability or responsibility for the accuracy, completeness, or any third party's use or the results of such use of any information, apparatus, product, or process disclosed, or represents that its use would not infringe privately owned rights. Reference herein to any specific commercial product, process, or service by trade name, trademark, manufacturer, or otherwise, does not necessarily constitute or imply its endorsement, recommendation, or favoring by the United States Government or any agency thereof or its contractors or subcontractors. The views and opinions of authors expressed herein do not necessarily state or reflect those of the United States Government or any agency thereof.

# **CsO<sub>x</sub> Nanostructures on Au(111): Morphology- and Size-dependent Activity for the Water-gas Shift Reaction**

Rui Shi<sup>1</sup>, Pedro J. Ramírez,<sup>2,3</sup> Rina Rosales,<sup>1</sup> Mausumi Mahapatra,<sup>4,5</sup> Ning Rui<sup>4</sup> and José A.  
Rodríguez<sup>\*,1,4</sup>

<sup>1</sup>Department of Chemistry, Stony Brook University, Stony Brook, New York 11794 (USA)

<sup>2</sup>Facultad de Ciencias, Universidad Central de Venezuela, Caracas 1020-A (Venezuela)

<sup>3</sup> Zoneca-CENEX, R&D Laboratories, Alta Vista, 64770 Monterrey (México)

<sup>4</sup>Chemistry Division, Brookhaven National Laboratory, Upton, New York 11973 (USA)

<sup>5</sup>Department of Chemistry & Biochemistry, Loyola University Chicago, Chicago, Illinois 60660 (USA)

\*To whom correspondence should be addressed, [rodriguez@bnl.gov](mailto:rodriguez@bnl.gov)

Tel. 631-344-2246

## Abstract

Alkali oxides are typically used as promoters of heterogeneous catalysts for the water-gas shift (WGS;  $\text{H}_2\text{O} + \text{CO} \rightarrow \text{H}_2 + \text{CO}_2$ ) reaction. On Au(111),  $\text{CsO}_x$  exhibits diverse nanostructures at varying coverages, as revealed by scanning tunneling microscopy. Clusters of cesium oxide ( $\text{Cs}_2\text{O}_2$ ) nucleate at elbow sites of the Au(111) herringbone when  $\theta_{\text{Cs}}$  is less than 0.1 ML. Subsequently, these clusters transform into two-dimensional (2D) islands ( $\text{Cs}_2\text{O}$ ,  $\text{Cs}_2\text{O}_2$ ,  $\text{CsO}_2$ ) as the cesium coverage increases ( $\theta_{\text{Cs}} > 0.1$  ML). Both types of  $\text{CsO}_x$  nanostructures enable the WGS process on Au(111). The highest activity was seen for the cesium oxide clusters which facilitated the partial dissociation of water and binding of CO. The  $\text{CO}_{\text{ads}}$  and  $\text{OH}_{\text{ads}}$  groups were not strongly bound and probably reacted to yield a short-lived HOCO intermediate that led to gaseous  $\text{H}_2$  and  $\text{CO}_2$ . The 2D islands of  $\text{CsO}_x$  also enabled the WGS but their efficiency was reduced due to the formation of cesium hydroxide compounds (limiting mobility of OH groups) and the generation of  $\text{CO}_3$  and C species (blocking of active centers). The fact that the performance of the  $\text{CsO}_x/\text{Au}(111)$  catalysts changed dramatically with variations in the chemical properties of the  $\text{CsO}_x$  nanostructures indicates that the alkali oxide was an integral part of the active phase, playing a central role in the activation and conversion of the reactants. To attach the label of “promoter” to  $\text{CsO}_x$  is a simplification that does not help in the design and optimization of catalysts for C1 chemistry. To achieve a rational design, one must consider the structural and chemical properties of the alkali oxide.

**Keywords:** Cesium oxide; Au(111); Carbon monoxide; Water ; Water-gas shift reaction; Hydrogen.

## I. Introduction

Cesium (Cs) and other alkali elements are typically added to metal/oxide catalysts to enhance their activity or selectivity.<sup>1,2,3,4</sup> Frequently, they are seen as promoters that modify the chemical properties of the metal or oxide phase by direct bonding or through-space interactions.<sup>1-4</sup> In a plain metal-alkali bond, the metal center receives electrons from the alkali (an electropositive element), and strong interactions can lead to a reconstruction of the metal surface or alloy formation.<sup>1-5,6</sup> Alkali atoms bound to oxide surfaces undergo rapid reduction and can exhibit high mobility.<sup>7,8,9,10</sup> They can exhibit a strong adsorption bond and a small barrier for surface diffusion on an oxide surface.<sup>8</sup>

In the case of the water-gas shift (WGS,  $\text{H}_2\text{O} + \text{CO} \rightarrow \text{H}_2 + \text{CO}_2$ ) reaction, it has been shown that the addition of an alkali enhances the activity of Cu(111),<sup>10,11,12</sup> and Cu(110),<sup>12,13</sup> Cu/ZnO,<sup>14</sup> Cu/Al<sub>2</sub>O<sub>3</sub>,<sup>15</sup> Cu/SiO<sub>2</sub>,<sup>1,16,17</sup> Pt/TiO<sub>2</sub><sup>16,17</sup> and Pt/CeO<sub>2</sub>.<sup>16,17</sup> The alkali can help with the most difficult step in the WGS process: The dissociation of water.<sup>10,11</sup> Promotion with Cs has been studied in detail.<sup>11,13-15,17</sup> The alkali adopts a CsO<sub>x</sub> composition under reaction conditions.<sup>11,13-15,17</sup> The oxidation state of the Cs is +1 but the exact number of oxygen atoms around the alkali center is usually unknown. This, and the fact that OH or carbonate groups could be bound to cesium cations, make it very difficult to define in a precise way the role of the alkali in the catalytic process.

In a recent study, we have used scanning tunneling microscopy (STM) and X-ray photoelectron spectroscopy (XPS) to examine the growth of nanostructures of CsO<sub>x</sub> on an inert support, Au(111).<sup>18</sup> STM images showed that at small coverages of the alkali, 0.05 - 0.10 monolayer (ML), clusters of Cs<sub>2</sub>O<sub>2</sub> nucleated at the elbows the Au(111) herringbone reconstruction, with medium size two-dimensional (2D) islands appearing at cesium coverages

above 0.15 ML.<sup>18</sup> The 2D islands “floated” on top of the gold terraces. XPS measurements revealed the existence of a suboxide ( $\text{Cs}_y\text{O}$ ;  $y \geq 2$ ) species within the island structures.<sup>18</sup> In this work, the  $\text{CsO}_x/\text{Au}(111)$  surfaces were used to test the intrinsic activity of the alkali oxide for the water-gas shift reaction. Our results show that small  $\text{CsO}_x$  clusters bind well to CO and are able to dissociate the water molecule into active OH groups. The corresponding  $\text{CsO}_x/\text{Au}(111)$  surfaces exhibit a WGS activity that is significantly larger than that of Cu(111), a typical benchmark in WGS studies.<sup>10-12,19</sup>

## II. Methods

### A. Scanning tunneling microscopy (STM).

The STM images were collected in an ultrahigh vacuum (UHV) system that has a base pressure of  $5 \times 10^{-10}$  Torr.<sup>18</sup> The STM instrument was built by SPECS Aarhus and it can be operated at variable temperature and near ambient pressure conditions.<sup>8,18</sup> In addition to the STM, the UHV chamber contained a quadrupole mass spectrometer, an ion gun for sputtering, and a Cs getter source. Circular Au(111) crystals (8-10 mm in diameter), cut to isolate the (111) surface plane within a tolerance of  $\pm 0.1^\circ$ , were used for the STM, XPS and catalytic studies. In general, sample cleaning consisted of cycles of sputtering with 1000 eV  $\text{Ar}^+$  ions at a surface temperature of 300 K, followed by annealing at 800 K in UHV.<sup>18</sup> On clean Au(111), cesium was deposited using a getter source at 300 K. The Cs/Au(111) systems were oxidized by exposing them to  $5 \times 10^{-7}$  Torr of  $\text{O}_2$  at 525 K for 10 min. Test experiments with XPS showed that these conditions were enough to reach saturation in the content of oxygen. A commercially etched tungsten tip was used for scanning and the images were collected under constant current mode. A code was used to estimate the  $\text{CsO}_x$  coverage by calculating the area of protruding features on the gold surface.

## **B. Ambient pressure X-ray photoelectron spectroscopy (AP-XPS).**

The CsO<sub>x</sub>/Au(111) surfaces were prepared following the same methodology used in the STM experiments.<sup>18</sup> The behavior of the samples under different gases (O<sub>2</sub>, H<sub>2</sub>O, CO) was investigated using commercial SPECS AP-XPS chambers, equipped with a PHOIBOS 150 EP MOD-9 analyzer and a Mg K $\alpha$  source. Spectra were collected for the O 1s, C 1s and Cs 3d regions. The binding energies were calibrated with respect to the position for the bulk 4f<sub>7/2</sub> peak of gold which was set at an energy of 84 eV.<sup>18,19</sup> Cesium and oxygen coverages for the CsO<sub>x</sub> species were estimate using the relative cross sections and sensitive factors of these elements and gold in XPS.<sup>20</sup> These coverages were used as a starting point to estimate the coverages of OH, CO and other C-containing species. In a test, the accuracy of this approach was verified by depositing O on Au(111) using ozone to generate an oxygen coverage of 1.2 ML<sup>19</sup> and obtain the corresponding O 1s /Au 4f signal ratio and then calibrate coverages for CsO<sub>x</sub>, OH, CO and CO<sub>3</sub> adsorbed species.

## **C. Catalytic tests**

The catalytic activity of the CsO<sub>x</sub>/Au(111) surfaces for the WGS reaction was examined using an apparatus that combines a main ultrahigh-vacuum (UHV) chamber (base pressure  $\sim 5 \times 10^{-10}$  Torr) for surface characterization and a functional batch reactor for kinetic tests.<sup>9,10,21</sup> Employing this apparatus, it was possible to transfer the sample under study back and forward between the reactor and UHV chamber without exposure to air.<sup>9,10,19</sup> The UHV chamber houses instrumentation for regular XPS, valence photoelectron spectroscopy (UPS), low-energy electron diffraction (LEED), ion scattering spectroscopy (ISS), and temperature programmed desorption (TDS).<sup>10,21</sup>

In the catalytic tests, the CsO<sub>x</sub>/Au(111) surfaces, after preparation and characterization, were moved into the batch reactor at room temperature, then the two reactant gases were

introduced (10 Torr of water and 20 Torr of carbon monoxide),<sup>10,21,25</sup> and the sample was rapidly heated to the desired reaction temperature (in the range of 550-625 K). Product buildup was monitored by gas chromatography (GC). The amount of molecules produced was normalized by the active area exposed by each sample.<sup>9,10,25</sup> Since Au(111) is not a catalyst for the WGS reaction,<sup>21,22</sup> only the front of the sample that contained CsO<sub>x</sub> was active and used for the normalization of the reaction rates. In our reactor a steady-state regime for the production of H<sub>2</sub> and CO<sub>2</sub> was reached after 2-3 minutes of reaction time.

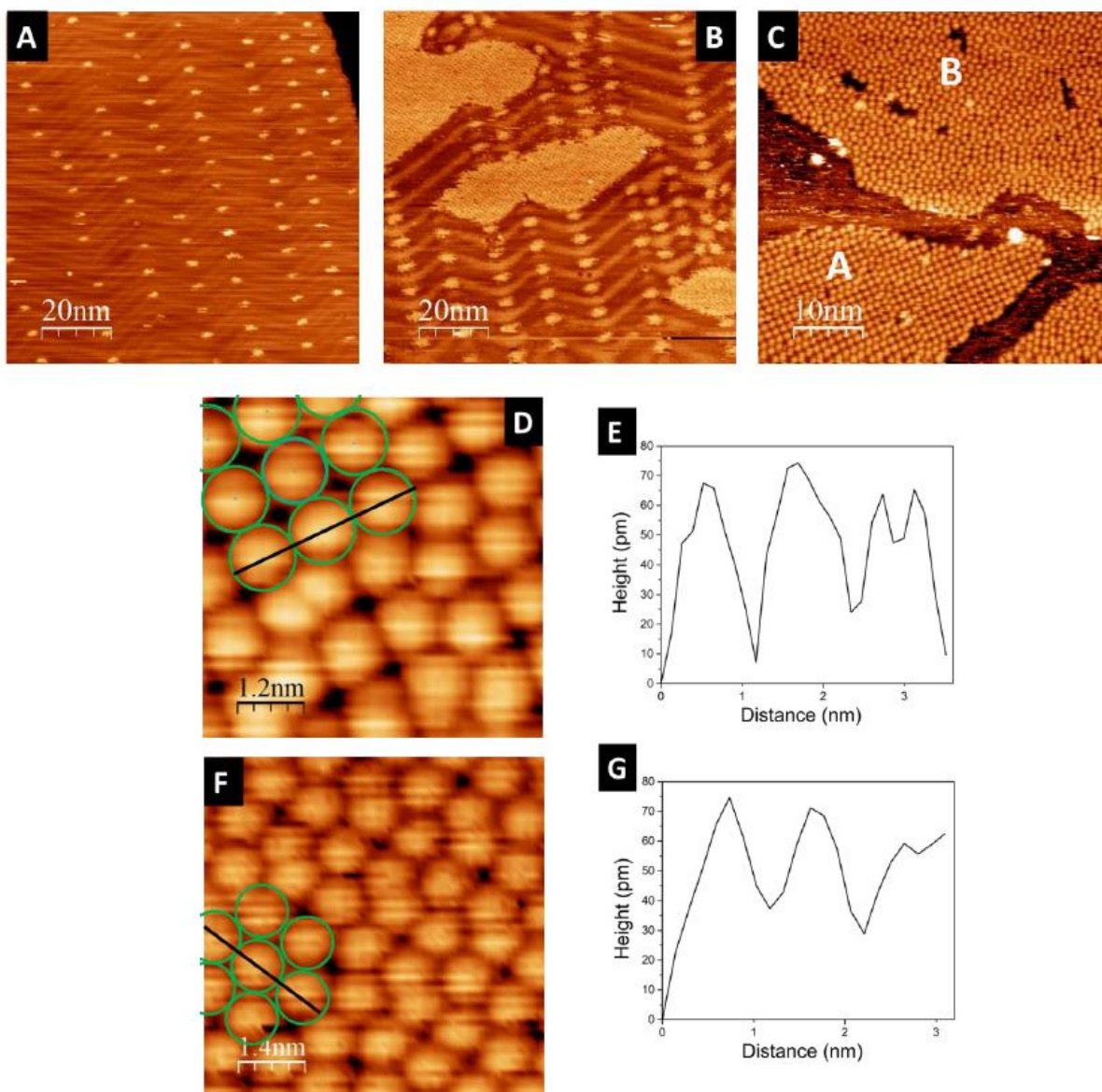
### III. Results and Discussion

#### A. Morphology and composition of the CsO<sub>x</sub>/Au(111) surfaces

Figure 1 displays images obtained with STM for 0.05 (A), 0.2 (B), and 0.6 ML (C) of CsO<sub>x</sub> on Au(111). The morphological characteristics for the CsO<sub>x</sub> coverages of 0.05 and 0.2 ML were analyzed in a previous work.<sup>18</sup> For the smallest alkali coverage (Figure 1A), clusters of Cs<sub>2</sub>O<sub>2</sub> are anchored on the elbows of the Au(111) herringbone, with a height of 1.5 Å and a width of 2.5 nm.<sup>18</sup> When the alkali coverage is increased to 0.2 ML (Figure 1B), 2D islands that contain Cs<sub>2</sub>O<sub>2</sub> and a Cs<sub>y</sub>O (y ≥ 2) suboxide appear.<sup>18</sup> These medium size islands (~ 60 nm long and ~ 20 nm wide) seem to be floating on top of the gold herringbone and the CsO<sub>x</sub> clusters.<sup>18</sup>

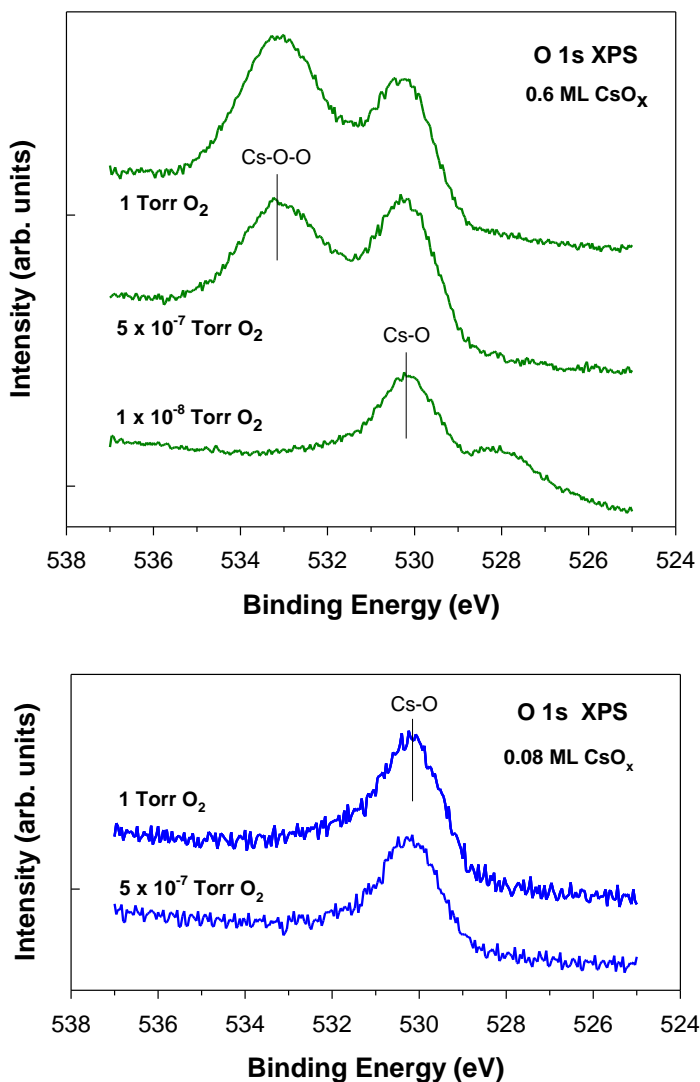
Figure 1C displays the morphology for a coverage of 0.6 ML of CsO<sub>x</sub>. The CsO<sub>x</sub> islands grow into a continuous film, covering most of the gold surface. Under these conditions, the tip of the STM cannot resolve well the underlying herringbone structure of Au(111). This structure may no longer exist at such a high coverage of CsO<sub>x</sub>. In Figure 1C, two different growth patterns (Zones A and B) can be observed on the surface. The atomic resolution of the STM image in Zone A is shown in Figure 1D, where a rectangular growth pattern is observed. By measuring the surface

corrugation (Figure 1E), the size of one bright dot appears to be  $\sim 1.2$  nm with an average height of  $\sim 0.7$  Å. A similar measurement was conducted on the hexagonal pattern in Zone B, as shown in Figure 1F,G, where the average size of one bright feature is also  $\sim 1.2$  nm with an average height  $\sim 0.7$  Å. The size ( $\sim 1.2$  nm) of one bright dot in these ordered patterns is consistent with the existence of  $(\text{CsO}_x)_n$  clusters within the film.



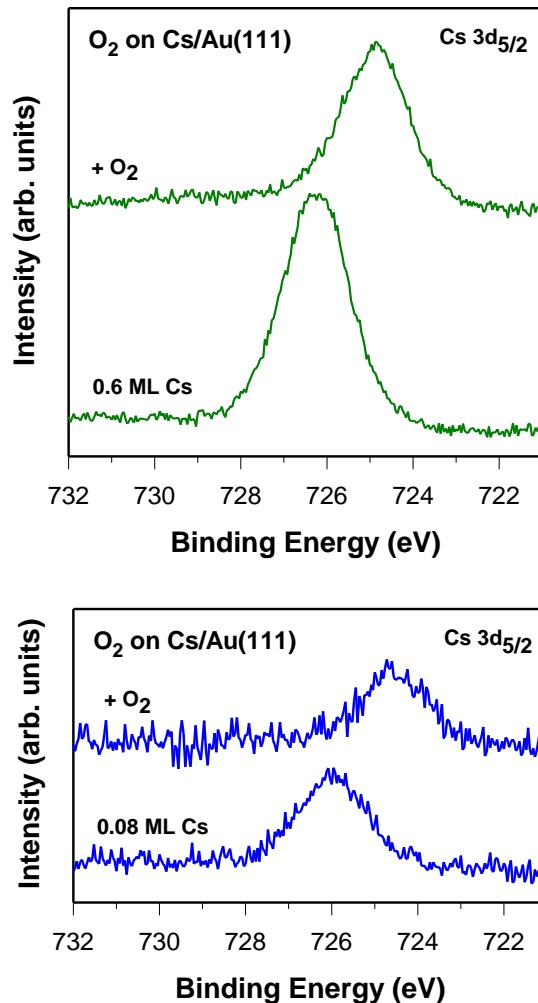
**Figure 1** STM images of CsO<sub>x</sub>/Au(111) (A) 0.05 ML, 100 nm×100 nm; (B) 0.2 ML, 100 nm×100 nm; (C) 0.6 ML, 50 nm×50 nm; (D) Atomic resolution image of zone A in panel C, 6 nm×6 nm; (E) Line profile along the line in (D); (F) Atomic resolution image of zone B in panel C, 6 nm×6 nm; (G) Line profile along the line in (F), V<sub>t</sub> = -1.8 V, I<sub>t</sub> = 0.2 nA for (A-C, D and F)

Figure 2 compares O 1s XPS spectra collected for surfaces with 0.08 and 0.6 ML of CsO<sub>x</sub>. O<sub>2</sub> does not dissociate on Au(111).<sup>19</sup> O atoms deposited on the gold substrate using ozone exhibit an O 1s peak at ~ 530 eV.<sup>19</sup> In the past, photoelectron spectroscopy has been used to examine the



**Figure 2** O 1s XPS spectra collected after dosing O<sub>2</sub> at 300 K to a Au(111) surface pre-covered with 0.08 (bottom panel) or 0.6 ML (top panel) of cesium. The pressure of O<sub>2</sub> was varied from 1 x 10<sup>-8</sup> to 1 Torr. oxidation of cesium multilayers, pointing to the formation of O-O-Cs, Cs-O-O-Cs, Cs-O, Cs-O-Cs and other suboxides.<sup>22,23</sup> Each one of these species was a well-defined position in the O 1s XPS region.<sup>22,23</sup> In the bottom of Figure 2, the surface with only 0.08 ML of cesium was rapidly saturated with oxygen and exhibits an O 1s peak at a binding energy of ~ 530.2 eV which indicates that the system has a Cs/O ratio close to 1/1 and Cs-O-O-Cs groups.<sup>22</sup> No other oxide or oxygen species was observed at O<sub>2</sub> pressures from 10<sup>-8</sup> to 1 Torr. The surface with a large coverage of Cs in the top panel of Figure 2 exhibits a behavior that resembles that of cesium multilayers:<sup>22</sup> Cs-O-O-Cs and a Cs<sub>y</sub>O (y ≥ 2) suboxide (at ~ 528 eV) are seen upon exposure to limited amounts of O<sub>2</sub> and the alkali is not fully oxidized, with O-O-Cs (at ~ 533 eV) and Cs-O-O-Cs (at ~ 530.2 eV) present when the system is saturated with oxygen.

An analysis of the Cs 3d core levels for these oxides showed a binding energy that was more than 1 eV smaller than that of metallic Cs (Fig. 3 and ref<sup>18</sup>). This negative shift agrees well with the trend seen for metallic cesium<sup>22</sup> and it reflects a big change in final state relaxation associated with a variation in the ionic Madelung field around the Cs species when is fully oxidized.<sup>22-24</sup> At the same time, there is a reduction of 10-15% in the intensity of the Cs core levels (Fig 3) that has been seen before<sup>18,22</sup> and comes from complex variations of the photoemission cross-section with the ionicity of the system.<sup>22-24</sup>



**Figure 3** Cs  $3d_{5/2}$  XPS spectra collected after dosing  $O_2$  at 300 K to a Au(111) surface pre-covered with 0.08 (bottom panel) or 0.6 ML (top panel) of cesium. The pressure of  $O_2$  was  $5 \times 10^{-7}$  Torr.

### B. Reaction with water: AP-XPS studies

The dissociation of water is usually seen as the rate determining step in the WGS reaction.<sup>10,11</sup> Au(111) is not able to dissociate the  $H_2O$  molecule.<sup>25,26</sup> Figure 4 shows O 1s AP-XPS spectra collected while exposing  $CsO_x/Au(111)$  surfaces to water at 300 or 400 K. The surfaces with 0.05 and 0.6 ML of  $CsO_x$  initially contained different oxygen species but reaction with water in both cases led to formation of Cs-OH (signal at  $\sim 531.3$  eV).<sup>27,28</sup> These hydroxyl groups did not disappear from the surface after evacuation of water from the gas phase at 300 or 400 K.

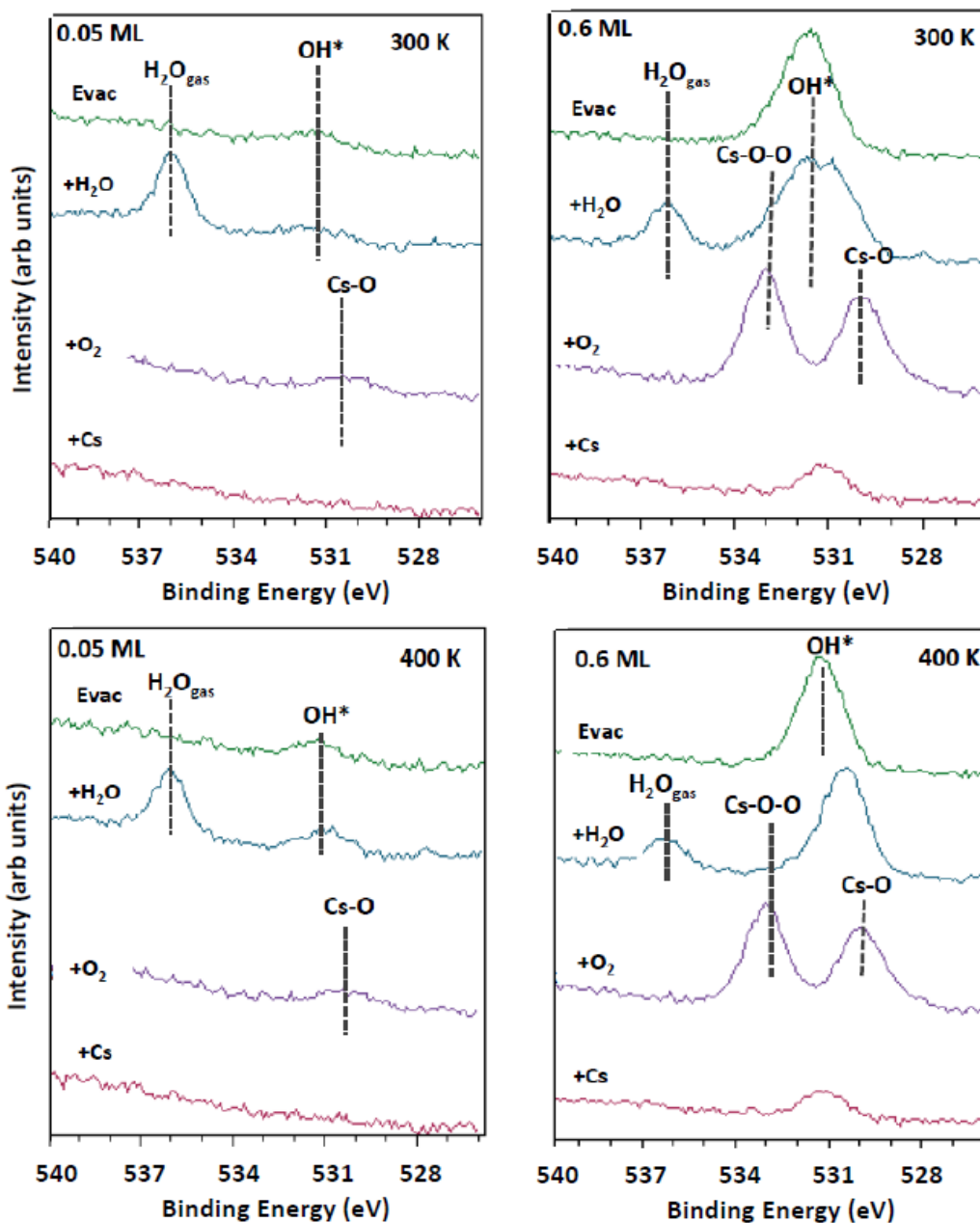


**Figure 4** O 1s XPS spectra for the exposure of CsO<sub>x</sub>/Au(111) surfaces, 0.05 and 0.6 ML of CsO<sub>x</sub>, to water at 300 (top panels) and 400 K (bottom panels). After depositing the Cs on the Au(111) substrate, the samples were oxidized under  $5 \times 10^{-7}$  Torr of O<sub>2</sub> at 300 K. Then, AP-XPS spectra were collected under 50 mTorr of H<sub>2</sub>O at 300 K (top panels), and the gas was removed in the final step. The panels at the bottom show a similar experiment with the exposure to water done at 400 K.

Figure 5 compares the stability of OH groups on 0.08 (nanoclusters in Figure 1A) and 0.6 ML (film in Figure 1C) of  $\text{CsO}_x$  on Au(111). For the surface with a low coverage of the alkali oxide, the OH groups started to disappear when the temperature of the sample was raised above 400 K. Most of the OH were labile but at 500-550 K some of these species still remained on the 0.08 ML

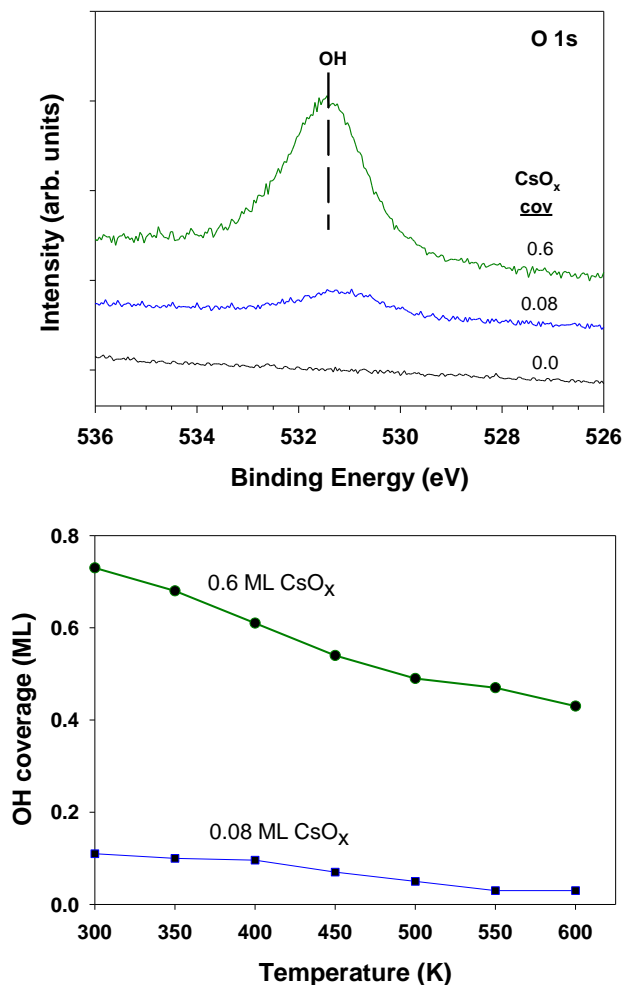


**Figure 5** O 1s XPS spectra collected after exposing clean Au(111), and  $\text{CsO}_x/\text{Au}(111)$  surfaces with 0.08 and 0.6 ML of  $\text{CsO}_x$  to 10 Torr of water at 300 K (top panel). Under vacuum the surfaces were heated from 300 to 600 K (bottom panel).

$\text{CsO}_x/\text{Au}(111)$  system. In the case of a high coverage of the alkali oxide, the removal of OH with increasing temperature was also seen. However, at 600 K, ~ 70% of the OH groups were still present. This is probably

a consequence of the formation of a bulk-like cesium hydroxide,<sup>29</sup> a compound that is commonly seen when water interacts with big chunks of cesium or cesium oxide. The removal of OH from Cs<sub>x</sub>OH compounds is not easy.<sup>29</sup> On the other hand, labile OH groups are a key factor for the formation of a HOCO intermediate,<sup>26,30,31</sup> which eventually leads to CO<sub>2</sub> and H<sub>2</sub> evolution, during the WGS process.

Figure 6 illustrates the effects of water adsorption on the Cs 3d core levels. The hydroxylation of the alkali oxide induced a positive binding energy shift (corresponding peak

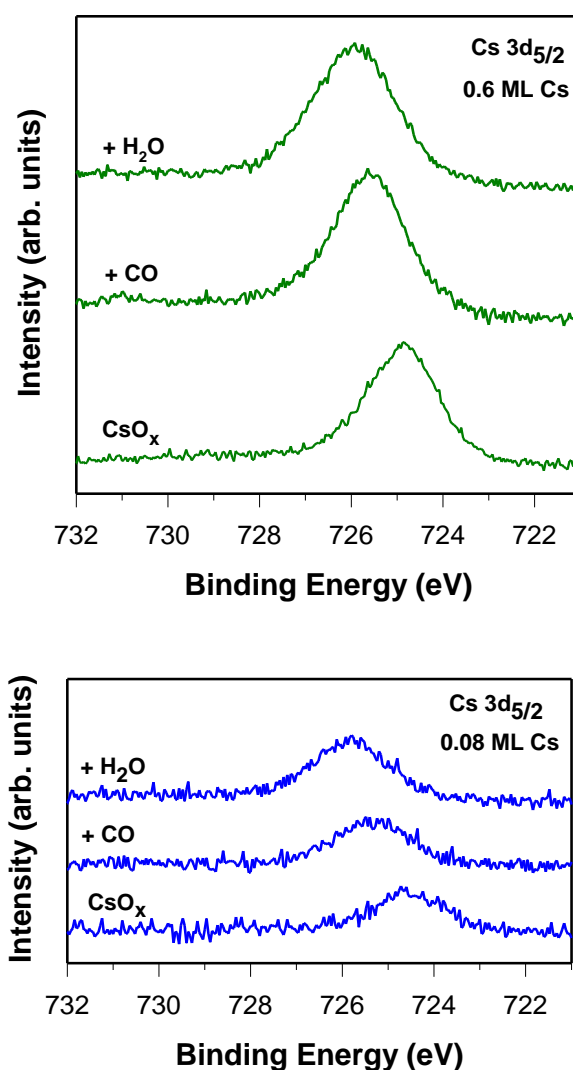


**Figure 6** Cs 3d<sub>5/2</sub> XPS spectra collected after exposing Au(111) surfaces pre-covered with 0.08 (bottom panel) and 0.6 ML (top panel) of CsO<sub>x</sub> to 10 Torr of water or 20 Torr of CO at 300 K. The gases were removed before collecting the spectra.

position of CsOH at ~ 726 eV)<sup>20</sup> that may reflect a decrease in the ionicity of the system.<sup>22-24</sup> At the same time, there was an enhancement (~ 10%) in the intensity of the Cs 3d features. These changes are consistent with a change in the structure of the alkali oxide nanostructures to allow direct bonding of the Cs cations to the OH groups. A similar phenomenon has been observed after doing CO<sub>2</sub> or H<sub>2</sub> to CsO<sub>x</sub>/Au(111) surfaces.<sup>18</sup> The geometry of the CsO<sub>x</sub> nanostructures is fluxional and varies with the chemical environment.<sup>18</sup>

### **C. Reaction with CO: AP-XPS studies**

Figure 7 displays C 1s XPS spectra recorded while exposing CsO<sub>x</sub>/Au(111) surfaces exposed to CO at 300 and 400 K. At temperatures above 200K, Au(111) does not bind CO<sup>25,26,32</sup> but the addition of cesium oxide produces systems that interact well with this molecule. On the surface with 0.08 ML of CsO<sub>x</sub>, the peak for chemisorbed CO appears at 286.4 eV.<sup>33</sup> It remains on the surface at 400 K when the gas is removed from the chamber and is gone by 500 K. This CO is bound stronger than on copper surfaces<sup>11,13,34</sup> but weaker than on late transition metals.<sup>33</sup> For a higher coverage of the alkali, in addition to adsorbed CO, one finds a strong peak for a carbonate, produced by the reaction of the adsorbate with O centers, and atomic carbon, coming from the full decomposition of the adsorbate. Thus, the film in Figure 1C exhibits chemical properties very different from those of the small clusters in Figure 1A.

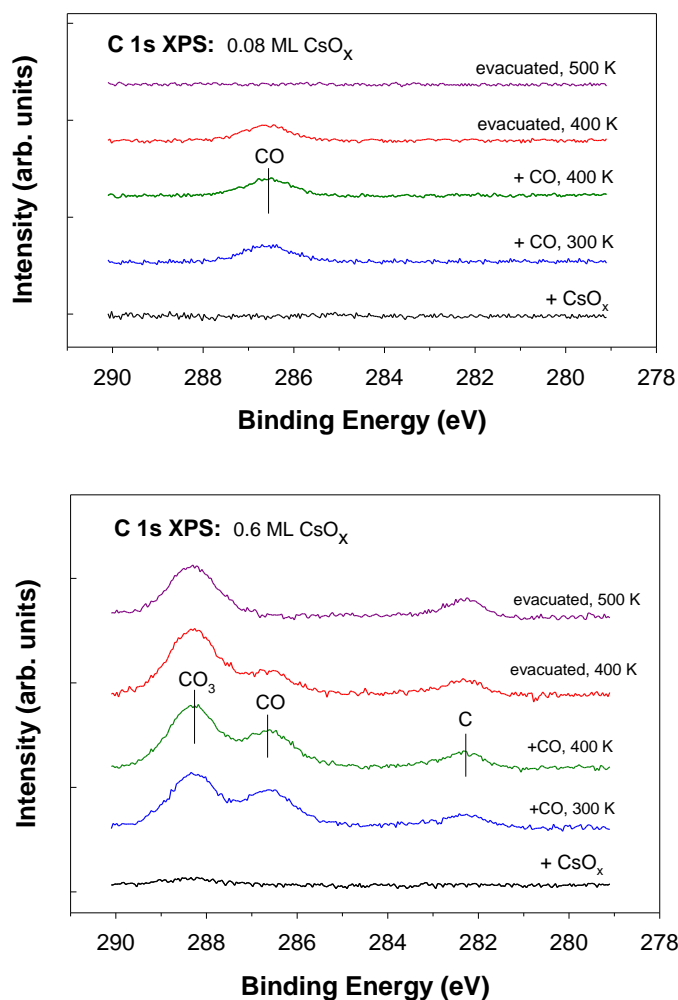


**Figure 7** C 1s XPS spectra collected while exposing CsO<sub>x</sub>/Au(111) surfaces with 0.08 (top panel) and 0.6 ML (bottom panel) of CsO<sub>x</sub> to 50 mTorr of CO at 300 or 400 K. In the final step, CO was removed from the chamber and spectra were collected at 400 and 500 K.

Figure 8 compares the thermal stability of the different C-containing species seen in Figure 7. On both CsO<sub>x</sub>/Au(111) surfaces, the binding of CO is reasonable if one is interested in performing the WGS reaction. Unfortunately, the CO<sub>3</sub> and C species present on the 0.6 ML CsO<sub>x</sub>/Au(111) system are problematic. Their concentration grows at high temperatures (> 450 K) and they can poison the WGS process.<sup>10,11</sup> The onset for the appearance of the medium-size islands

of  $\text{CsO}_x$  in Figure 1B was also the onset for the generation of  $\text{CO}_3$  and C on the samples. After that point, the larger the amount of alkali dispersed on the sample, the faster the generation of C-spurious species.

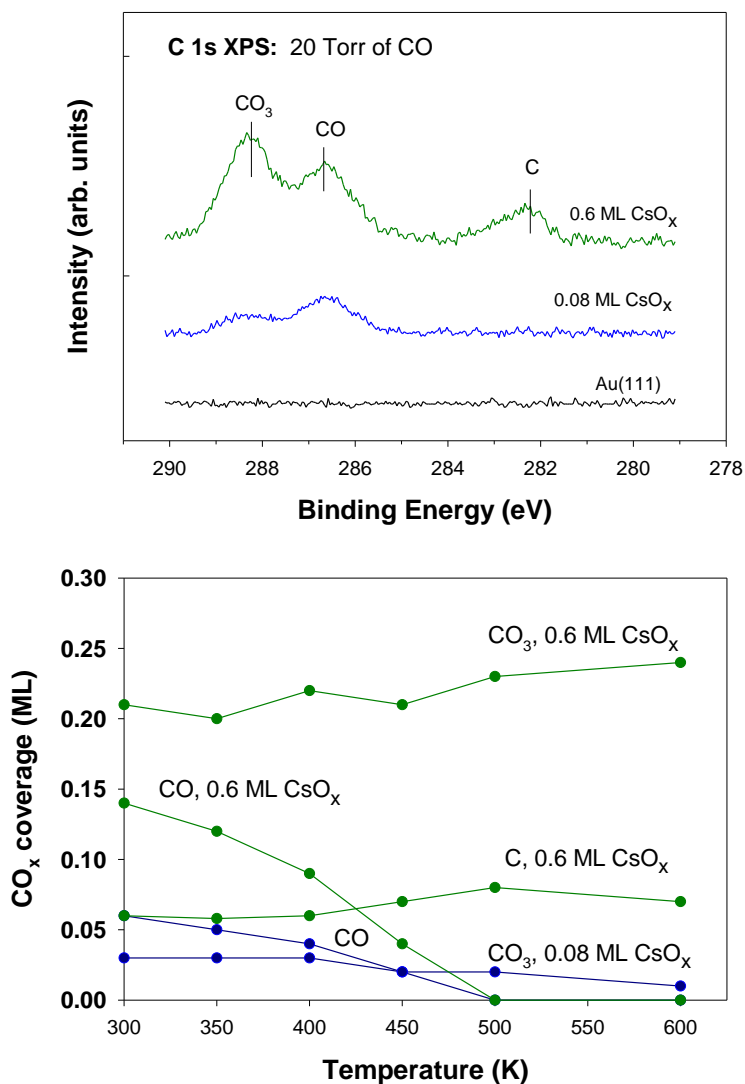
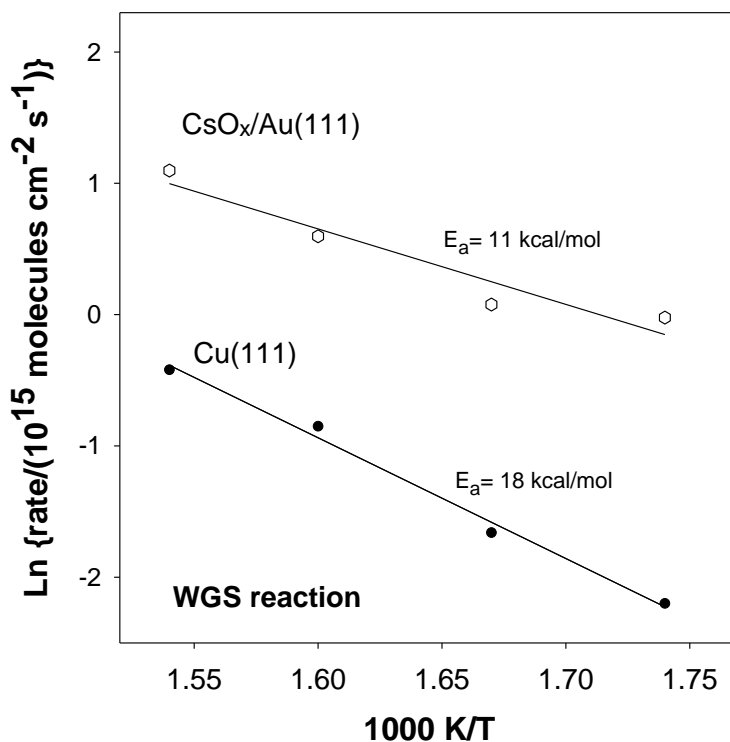


**Figure 8** C 1s XPS spectra collected after exposing clean Au(111), and  $\text{CsO}_x/\text{Au}(111)$  surfaces with 0.08 and 0.6 ML of  $\text{CsO}_x$  to 20 Torr of CO at 300 K (top panel). Under vacuum the surfaces were heated from 300 to 600 K (bottom panel).

In Figure 6, exposure to CO reduces the binding energy and increases the intensity of the Cs 3d<sub>5/2</sub> core level. As happened in the case of H<sub>2</sub>O adsorption, here, there is also a geometrical change in the CsO<sub>x</sub> nanostructures that facilitates binding of the Cs cations to CO, or the formed CO<sub>3</sub> and C products. The XPS results in Figure 4-8 indicate that alkali centers can be quite active for bonding and activating the reactants of the WGS reaction.

#### D. Catalytic activity of CsO<sub>x</sub>/Au(111) for the WGS

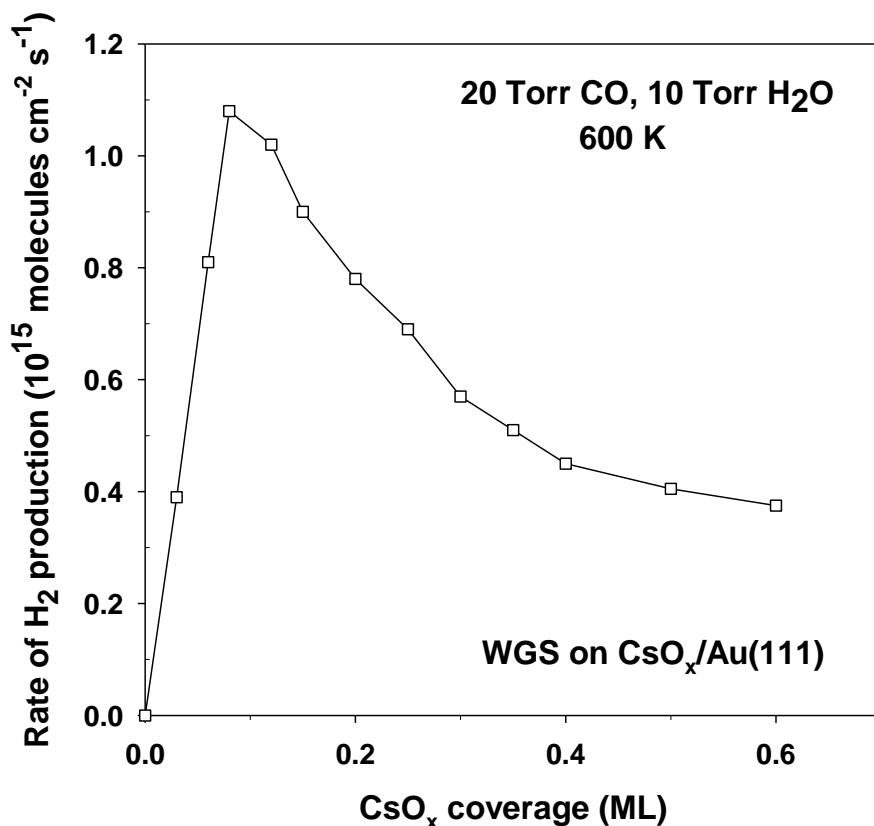
Au(111) is inert as a catalyst for the WGS reaction.<sup>25,26</sup> The addition of a small coverage of CsO<sub>x</sub> (0.08 ML) to the gold substrate facilitates the dissociation of water and binding of CO, producing a very good WGS catalyst. Figure 9 shows an Arrhenius plot displaying the activity of this CsO<sub>x</sub>/Au(111) catalyst at temperatures between 575 and 650 K. The CsO<sub>x</sub>/Au(111) surface is always more active than Cu(111), a typical benchmark catalyst for the WGS process.<sup>10-12,30</sup> The



**Figure 9** Arrhenius plots for the WGS reaction on Cu(111) and on a Au(111) surface pre-covered with 0.08 ML of CsO<sub>x</sub> (P<sub>CO</sub>= 20 Torr; P<sub>H<sub>2</sub>O</sub> = 10 Torr).

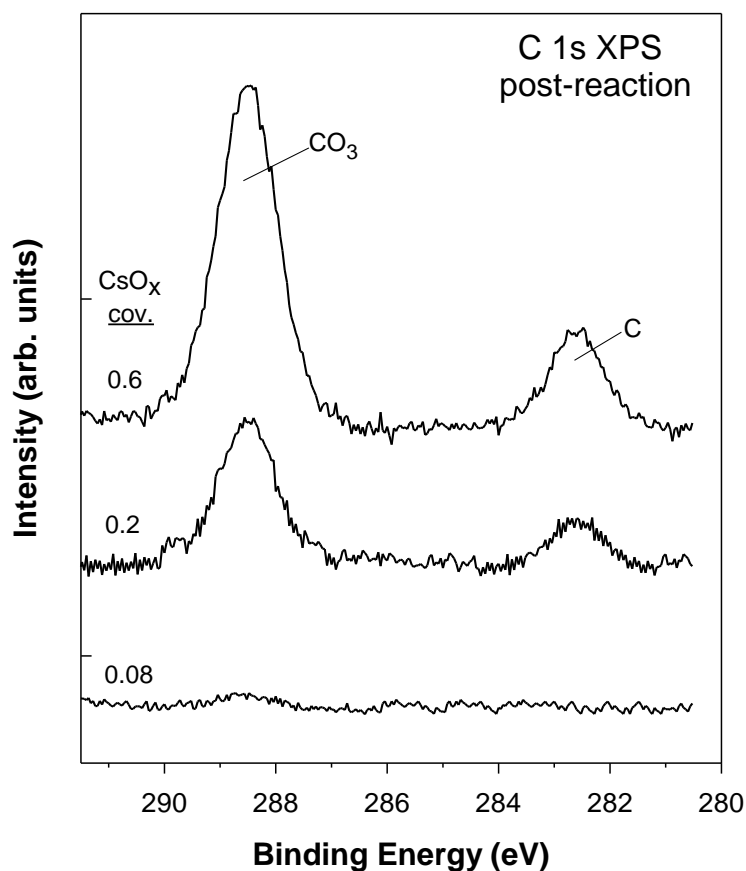
apparent activation energy goes from 18 kcal/mol on Cu(111) to 11 kcal/mol on CsO<sub>x</sub>/Au(111). This decrease probably reflects a better interaction with the reactants in the case of the alkali containing catalyst.

Figure 10 displays the catalytic activity of CsO<sub>x</sub>/Au(111) surfaces as a function of alkali oxide coverage. As CsO<sub>x</sub> is added to the gold substrate, there is an increase in the rate of H<sub>2</sub> production until a maximum is found near 0.1 ML. At these small alkali coverages, CsO<sub>x</sub> clusters occupy the elbows of the gold herringbone (Figure 1A) and there are no strong bonds with CO (Figure 8) or the OH generated by water dissociation (Figure 5). The CO<sub>ads</sub> and OH<sub>ads</sub> could react to yield a short-lived HOCO intermediate that would lead to gaseous H<sub>2</sub> and CO<sub>2</sub>.<sup>24,30,31,35</sup>



**Figure 10** Production of H<sub>2</sub> through the WGS reaction on CsO<sub>x</sub>/Au(111) surfaces as a function of alkali oxide coverage (T= 600 K; P<sub>CO</sub>= 20 Torr; P<sub>H<sub>2</sub>O</sub>= 10 Torr).

At CsO<sub>x</sub> coverages above 0.1 ML, 2D islands of the alkali oxide start to grow (Figure 1B and ref. <sup>18</sup>), and there is a change in the chemical properties of the system that leads to the drop in activity seen in Figure 8. The OH groups of a cesium hydroxide are not labile (Figure 5) and CO<sub>3</sub> and C (Figure 8) block active sites on the surface. Figure 11 shows C 1s XPS spectra measured after performing the WGS on three CsO<sub>x</sub>/Au(111) surfaces. In the spectrum for 0.08 ML of CsO<sub>x</sub>, the maximum of activity in Figure 10, the surface is essentially clean of C-containing species. There is a very



**Figure 11** C 1s XPS spectra recorded after carrying out the WGS reaction on three different CsO<sub>x</sub>/Au(111) surfaces (T= 600 K; P<sub>CO</sub>= 20 Torr; P<sub>H<sub>2</sub>O</sub>= 10 Torr). At 600 K, the gases were pumped out from the reactor and the samples were cooled down (T < 400 K) before collecting the C 1s spectra.

small feature near 288.5 eV that could be attributed to a trace ( $< 0.05$  ML) of  $\text{CO}_3$ . This feature grows in intensity and dominates the C 1s spectra for 0.2 and 0.6 ML of  $\text{CsO}_x$ . It is known that carbonates bound to alkali cations deactivate WGS catalysts.<sup>10,11</sup>

In experiments of AP-XPS performed with moderate pressures of the WGS reactants (25 mTorr of  $\text{H}_2\text{O}$ ; 25 mTorr of  $\text{CO}$ ), we found that  $\text{CO}$  was adsorbed on the surface at 450 K but no trace was found for the molecule at 600 K (see Figure 12). At this high temperature the residence time of  $\text{CO}$  on the surface is very small but the activation barrier for the  $\text{CO}_{\text{ads}} + \text{OH}_{\text{ads}} \rightarrow \text{CO}_{2,\text{gas}} + 0.5\text{H}_{2,\text{gas}}$  reaction<sup>30,31</sup> is probably overcome faster. The surface with 0.08 ML of  $\text{CsO}_x$  was free of  $\text{CO}_3$  and C species, but they were present on the surface with 0.6 ML of  $\text{CsO}_x$  (top of Figure 12). This agrees well with the XPS spectra collected after performing the WGS reaction at larger reactant pressure (Figure 11).

The chemistry and catalysis observed in Figures 4-12 could take place on the  $\text{CsO}_x$  nanostructures or on the  $\text{CsO}_x$ -Au interface. The trends seen in Figure 6 for changes in the Cs 3d<sub>5/2</sub> core level indicate that the alkali interacts well with  $\text{CO}$  and water. Au(111) and Au(100) do not dissociate water but can perform other steps associated with the WGS reaction.<sup>26,35,36</sup> The addition of nanoparticles of  $\text{CeO}_x$ ,<sup>25</sup>  $\text{TiO}_x$ ,<sup>25</sup>  $\text{SnO}_x$ ,<sup>37</sup> and  $\text{InO}_x$ <sup>38</sup> to Au(111) produces active oxide-metal interfaces for the WGS and C1 chemistry. The same could be happening in the case of the  $\text{CsO}_x$  nanostructures. The significant variation in the performance of the  $\text{CsO}_x/\text{Au}(111)$  catalysts with changes in the chemical properties of the  $\text{CsO}_x$  nanostructures underscores the vital role of the alkali oxide in the activation and conversion of the reactants. Characterizing  $\text{CsO}_x$  simply as a "promoter" oversimplifies its contribution and does not aid in the design and optimization of catalysts for C1 chemistry. Any approach for a rational design must consider the structural and chemical properties of the alkali oxide.

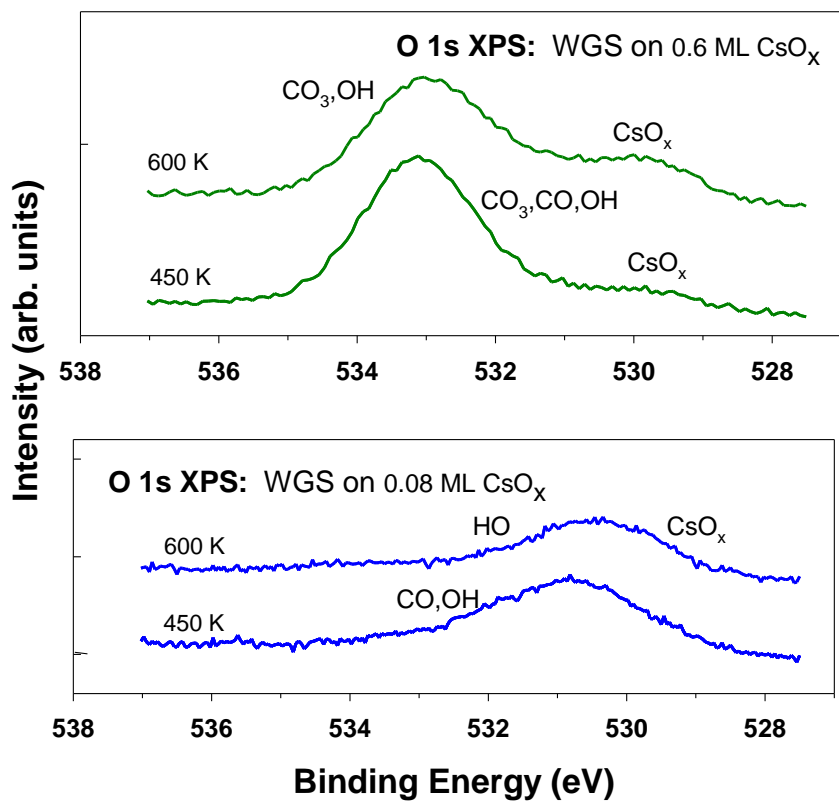
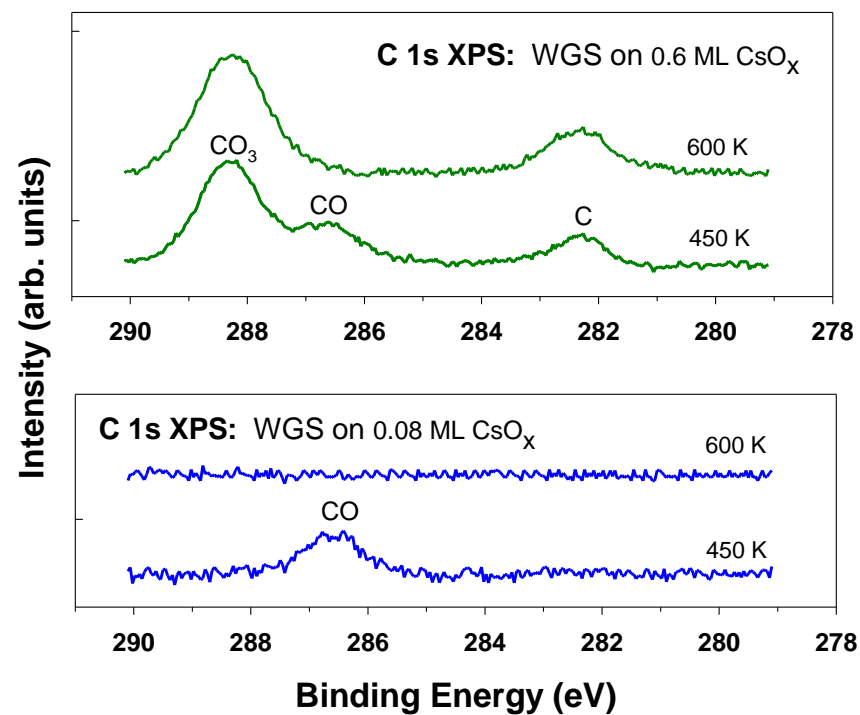


**Figure 12** C 1s (top panels) and O 1s (bottom panels) AP-XPS spectra collected while exposing CsO<sub>x</sub>/Au(111) surfaces to 25 mTorr of CO and 25 mTorr of H<sub>2</sub>O at 450 and 600 K. The Au(111) surface was pre-covered with 0.08 and 0.6 ML of CsO<sub>x</sub>.

#### 4. Conclusions

CsO<sub>x</sub> nanostructures enable the WGS process on Au(111). The highest catalytic activity is seen for surfaces with small cesium oxide clusters (~ 2.5 nm in size) which facilitate the partial dissociation of water and binding of CO. The CO<sub>ads</sub> and OH<sub>ads</sub> generated are not strongly bound and probably react to yield a short-lived HOCO intermediate that leads to gaseous H<sub>2</sub> and CO<sub>2</sub>. 2D islands of CsO<sub>x</sub> (> 20 nm in size) also enable the WGS but their efficiency is reduced due to the formation of cesium hydroxide compounds (limiting mobility of OH groups) and the generation of CO<sub>3</sub> and C species (blocking of active centers). Our results indicate that cesium oxide is not a plain “promoter.” It is an integral part of the catalyst active phase. Its structural and chemical properties must be considered when doing a rational design or optimization of catalysts for the WGS and C1 chemistry.

#### Acknowledgement

The research done at the Chemistry Division of Brookhaven National Laboratory was supported by the U.S. Department of Energy, Office of Science, Office of Basic Energy Sciences, Chemical Sciences, Geosciences, and Biosciences Division, Catalysis Science Program (Grant No DE-SC0012704). PJR is grateful to Zoneca-CENEX for an internal grant that made possible part of this research. The authors thank Vikram Mehar for his help when examining water adsorption.

#### References

- 
- <sup>1</sup> Bonzel, H. P., Alkali-metal-affected Adsorption of Molecules on Metal Surfaces. *Surf. Sci. Reports* **1988**, 8 (2), 43-125.
- <sup>2</sup> Campbell, C. T., Ultrathin Metal Films and Particles on Oxide Surfaces: Structural, Electronic and Chemisorptive Properties. *Surf. Sci. Reports* **1997**, 27 (1), 1-111.
- <sup>3</sup> Koel, B. E.; Kim, J., Promoters and Poisons. In *Handbook of Heterogeneous Catalysis*, Ertl G., Knözinger H., Schüth F., Weitkamp J., Editors; Weinheim: Wiley-VCH, 2008.
- <sup>4</sup> Farkas, A. P.; Solymosi, F., Activation and Reactions of CO<sub>2</sub> on a K-Promoted Au(111) Surface. *J. Phys. Chem. C* **2009**, 113 (46), 19930-19936.
- <sup>5</sup> Häberle, P.; Fenter, P.; Gustafsson, T., Structure of the Cs-induced (1 x 3) Reconstruction of Au(110). *Phys. Rev. B* **1989**, 39 (9), 5810-5818.
- <sup>6</sup> Barth, J. V.; Schuster, R.; Behm, R. J.; Ertl, G., The system K/Au(111): Adsorption and Surface Restructuring. *Surf. Sci.* **1996**, 348 (3), 280-286.
- <sup>7</sup> Bedrow, T.; Aprà, E.; Catti, M.; Pacchioni, G. Cluster and Periodic Ab-initio Calculations on K/TiO<sub>2</sub>(110). *Surf. Sci.* **1998**, 418 (2), 150-165.
- <sup>8</sup> Grinter, D.C.; Remesal, E.R.; Luo, S.; Evans, J.; Senanayake, S.D.; Stacchiola, D.J.; Graciani, J.; Fernández-Sanz, J.; Rodriguez, J.A. Potassium and Water Co-adsorption on TiO<sub>2</sub>(110): OH-Induced Anchoring of Potassium and the Generation of Single-Site Catalysts, *J. Phys. Chem. Lett.* **2016**, 7 (19), 3866–3872.
- <sup>9</sup> Wang, X.; Ramírez, P. J.; Liao, W.; Rodriguez, J. A.; Liu, P., Cesium-Induced Active Sites for C–C Coupling and Ethanol Synthesis from CO<sub>2</sub> Hydrogenation on Cu/ZnO(000 $\bar{1}$ ) Surfaces. *Journal of the American Chemical Society* **2021**, 143 (33), 13103-13112.
- <sup>10</sup> Rodriguez, J. A.; Remesal, E. R.; Ramírez, P. J.; Orozco, I.; Liu, Z.; Graciani, J.; Senanayake, S. D.; Sanz, J. F., Water–Gas Shift Reaction on K/Cu(111) and Cu/K/TiO<sub>2</sub>(110) Surfaces: Alkali Promotion of Water Dissociation and Production of H<sub>2</sub>. *ACS Catal.* **2019**, 9 (12), 10751-10760.
- <sup>11</sup> Campbell, C.T.; Koel, B.E. A Model Study of Alkali Promotion of Water-gas Shift Catalysts: Cs/Cu(111), *Surf. Sci.* **1987**, 186 (3), 393-411.
- <sup>12</sup> Wang, Y.-X.; Wang, G.-C.; A Systematic Theoretical Study of Water Gas Shift Reaction on Cu(111) and Cu(110): Potassium Effect, *ACS Catal.* **2019**, 9 (3), 2261–2274.
- <sup>13</sup> Campbell, J. M.; Nakamura, J.; Campbell, C. T., Model Studies of Cesium Promoters in Water-gas Shift Catalysts: Cs/Cu(110). *J. Catal.* **1992**, 136 (1), 24-42.

- 
- <sup>14</sup> Klier, K.; Young, C. W.; Nunan, J. G., Promotion of the Water-gas Shift Reaction by Cesium Surface doping of the Model binary Copper/Zinc Oxide Catalyst. *Ind. & Eng. Chem. Fundamentals* **1986**, *25* (1), 36-42.
- <sup>15</sup> Amenomiya, Y.; Pleizier, G. Alkali-promoted Alumina Catalysts: II. Water-gas Shift Reaction, *J. Catal.* **1982**, *76* (2), 345-353.
- <sup>16</sup> Yang, M.; Liu, J.; Lee, S.; Zugic, B.; Huang, J.; Allard, L. F.; Flytzani-Stephanopoulos, M., A Common Single-Site Pt(II)–O(OH)<sub>x</sub>– Species Stabilized by Sodium on “Active” and “Inert” Supports Catalyzes the Water-Gas Shift Reaction. *Journal of the American Chemical Society* **2015**, *137* (10), 3470-3473.
- <sup>17</sup> Ebrahimi, P.; Kumar, A.; Khraisih, M. A Review of Recent Advances in Water-gas shift Catalysis for Hydrogen Production, *Emergent Materials*, **2020**, *3* (2), 881-917.
- <sup>18</sup> Mehar, V.; Liao, W.; Mahapatra, M.; Shi, R.; Lim, H.; Barba-Nieto, I.; Hunt, A.; Waluyo, I.; Liu P.; Rodriguez, J.A. Morphology Dependent Reactivity of CsO<sub>x</sub> Nanostructures on Au(111): Binding and Hydrogenation of CO<sub>2</sub> to HCOOH, *ACS Nano*, **2023**, *17* (22), 22990-22998.
- <sup>19</sup> Saliba, N.; Parker, D.H.; Koel, B.E. Adsorption of Oxygen on Au(111) by Exposure to Ozone, *Surf. Sci.* **1998**, *410* (3), 270-282.
- <sup>20</sup> Wagner, C.D.; Davis, L.E.; Zeller, M.V. ; Taylor, J.A.; Raymond, R.H.; Gale, L.H. Empirical Atomic Sensitivity Factors for Quantitative Analysis by Electron Spectroscopy for Chemical Analysis, *Surface and Interface Analysis*, **1981**, *3* (5), 211-225.
- <sup>21</sup> Rodriguez, J.A.; Liu, P.; Hrbek, J.; Evans, J.; Perez, M. Water-gas Shift Reaction on Cu and Au Nanoparticles Supported on CeO<sub>2</sub>(111) and ZnO(0001): Intrinsic Activity and Importance of Support Interactions. *Ang. Chem. Int. Ed.* **2007**, *46* (8), 1329-1332
- <sup>22</sup> Hrbek, J.; Yang, Y. W.; Rodriguez, J. A., Oxidation of Cesium Multilayers. *Surf. Sci.* **1993**, *296* (2), 164-170.
- <sup>23</sup> Jupille, J.; Dolle, P.; Besançon, M., Ionic Oxygen Species Formed in the Presence of Lithium, Potassium and Cesium. *Surf. Sci.* **1992**, *260* (1), 271-285.
- <sup>24</sup> Egelhoff, W. F., Core-level Binding-energy Shifts at Surfaces and in Solids. *Surf. Sci. Reports* **1987**, *6* (6), 253-415.
- <sup>25</sup> Rodriguez, J.A.; Ma, S.; Hrbek, J.; Evans, J.; Pérez, M. Activity of CeO<sub>x</sub> and TiO<sub>x</sub> Nanoparticles Grown on Au(111) in the Water-gas Shift Reaction, *Science*, *318* (5857), 1757-1760.
- <sup>26</sup> Liu, P.; Rodriguez, J.A. Water-gas Shift Reaction on Metal Nanoparticles and Surfaces, *J. Chem. Phys.* **2007**, *126*, 164705.

- 
- <sup>27</sup> Carrasco, J.; López-Durán, D.; Liu, Z.; Duchoň, T.; Evans, J.; Senanayake, S.D.; Crumlin, E.J.; Matolín, V.; Rodríguez, J.A.; Ganduglia-Pirovano, M.V. In-situ and Theoretical Studies for the Dissociation of Water on an Active Ni/CeO<sub>2</sub> Catalyst: Importance of Strong Metal–support Interactions for the Cleavage of O–H Bonds. *Angew. Chem. Int. Ed.* **2015**, *54* (13), 3917–3921.
- <sup>28</sup> Idriss, H. On the Wrong Assignment of the XPS O1s signal at 531–532 eV Attributed to Oxygen Vacancies in Photo- and Electro-catalysts for Water Splitting and other Materials Applications, *Surf. Sci.* **2021**, *712*, 121894.
- <sup>29</sup> Gurvich, L.V.; Bergman, G.A.; Gorokhov, L.N.; Iorish, V.S.; Ya, V.; Leonidov, Ya.; Yungman, V.S. Thermodynamic Properties of Alkali Metal Hydroxides. Part II. Potassium, Rubidium, and Cesium Hydroxides, *J. Phys. & Chem. Reference Data*, **1997**, *26*, 1031-1110.
- <sup>30</sup> Gokhale, A. A.; Dumesic, J. A.; Mavrikakis, M. On the Mechanism of Low-Temperature Water Gas Shift Reaction on Copper. *J. Am. Chem. Soc.* **2008**, *130* (4), 1402–1414.
- <sup>31</sup> Rodríguez, J.A.; Evans, J.; Graciani, J.; Park, J.-B.; Liu, P.; Hrbek, J.; Sanz, J.F. High Water-Gas Shift Activity in TiO<sub>2</sub>(110) Supported Cu and Au Nanoparticles: Role of the Oxide and Metal Particle Size. *J. Phys. Chem. C*, **2009**, *113* (17), 7364-7370.
- <sup>32</sup> Thuening, T.; Walker, J.; Adams, H.; Furlong, O.; Tysoe, W. Kinetics of Low Temperature CO Oxidation on Au(111), *Surf. Sci.* **2016**, *648* (1), 236-241.
- <sup>33</sup> Toyoshima, R.; Yoshida, M.; Monya, Y.; Suzuki, K.; Amemiya, K.; Mase, K.; Mun, B.S.; Kondoh, H. A High-pressure-induced Dense CO Overlayer on a Pt(111) Surface: A Chemical Analysis using *In-situ* near Ambient Pressure XPS, *Phys. Chem. Chem. Phys.* **2014**, *16*, 23564-23567.
- <sup>34</sup> Rodríguez, J. A.; Clendening, W. D.; Campbell, C. T. Adsorption of CO and CO<sub>2</sub> on Clean and Cesium-Covered Cu(110). *J. Phys. Chem.* **1989**, *93*, 5238– 5248.
- <sup>35</sup> Kim, T.S.; Gong, J.; Ojifinmi, R.A.; White, J.M.; Mullins, C.B. Water Activated by Atomic Oxygen on Au(111) to Oxidize CO at Low Temperatures, *J. Am. Chem. Soc.* **2006**, *128* (19), 6282–6283.
- <sup>36</sup> Gong, J.; Ojifinmi, R.A.; Kim, T.S.; Stiehl, J.D.; McClure, S.M.; White, J.M.; Mullins, C.B. Low Temperature CO Oxidation on Au(111) and the Role of Adsorbed Water, *Topics in Catal.* **2007**, *44* (1), 57-63.
- <sup>37</sup> Kang, J.; Rui, N.; Rosales, R.; Tian, Y.; Senanayake, S.D.; Rodríguez, J.A. Understanding the Surface Structure and Catalytic Activity of SnO<sub>x</sub>/Au(111) Inverse Catalysts for CO<sub>2</sub> and H<sub>2</sub> Activation, *J. Phys. Chem. C* **2022**, *126*, 10, 4862–4870.
- <sup>38</sup> Kang, J.; Mahapatra, M.; Rui, N.; Orozco, I.; Shi, R.; Senanayake, S.D.; Rodríguez, J.A. Growth and Structural Studies of In/Au(111) Alloys and InO<sub>x</sub>/Au(111) Inverse Oxide/metal Model Catalysts, *J. Chem. Phys.* **2020**, *152*, 054702.

---

TOC

